Dissociation and Redistribution of Na^+,K^+-ATPase from Its Surface Membrane Actin Cytoskeletal Complex during Cellular ATP Depletion

B. A. Molitoris,* A. Geerdes,* J. R. McIntosh‡

*Departments of Medicine and Cellular and Structural Biology, University of Colorado, School of Medicine, Denver, Colorado 80262; ‡Department of Molecular, Cellular, and Developmental Biology, University of Colorado, Boulder, Colorado 80309

Abstract

Establishment and maintenance of a polar distribution of Na^+,K^+-ATPase is essential for efficient Na^+ reabsorption by proximal tubule cells and is dependent upon the formation of a metabolically stable, detergent-insoluble complex of Na^+,K^+-ATPase with the actin membrane cytoskeleton. The present studies show that cellular ATP depletion results in a rapid duration-dependent dissociation of Na^+,K^+-ATPase from the actin cytoskeleton and redistribution of Na^+,K^+-ATPase to the apical membrane. During ATP depletion, total cellular Na^+,K^+-ATPase activity was unaltered, but the Triton-X-100–insoluble fraction (cytoskeleton associated) of Na^+,K^+-ATPase activity decreased ($P < 0.01$), with a corresponding increase in the detergent-soluble fraction of Na^+,K^+-ATPase ($P < 0.01$). Indirect immunofluorescent studies of cells with depleted ATP revealed a redistribution of Na^+,K^+-ATPase from the basolateral membrane into the apical membrane and throughout the cytoplasm. ATP depletion also resulted in the redistribution of F-actin from a primarily cortical concentration to a perinuclear location. There was also a rapid, duration-dependent conversion of monomeric G-actin to F-actin starting during the first 5 min of ATP depletion. Taken together, these data suggest that ATP depletion causes profound alterations in cell polarity by inducing major changes in the actin cytoskeletal architecture. (*J. Clin. Invest.* 1991. 88:462–469.) Key words: epithelial polarity • cytoskeleton • ankyrin ischemia • acute renal failure

Introduction

A polar distribution of Na^+,K^+-ATPase is essential for efficient movement of Na^+ across epithelial cells. After synthesis, Na^+,K^+-ATPase is targeted in a polar fashion to the basolateral membrane (BLM)[1] (1), where it forms a metabolically stable, detergent-insoluble complex with elements of the actin membrane-cytoskeleton (2–4). Na^+,K^+-ATPase binds directly to ankyrin (4–6) via its α subunit (5). Madin-Darby canine kidney (MDCK) cells plated as monolayers display a gradual shift in the location of Na^+,K^+-ATPase from a previously random distribution over the entire surface membrane to an accumulation in the BLM. This emergence of cell polarity is dependent upon cell–cell contact and the uvomorulin-mediated assembly and organization of a basolateral membrane cytoskeleton (3, 7).

We have previously reported that during in vivo ischemia, renal proximal tubular cells undergo a rapid loss of surface membrane protein and lipid polarity whose extent depends on the duration of treatment. Both biochemical and histochemical evidence show that Na^+,K^+-ATPase redistributes during ischemia from the basolateral membrane into the apical membrane domain (8, 9). Loss of Na^+,K^+-ATPase surface membrane polarity is associated with reduced proximal tubular Na^+ reabsorption (10). Upon reperfusion the situation normalizes during cellular repair with the reestablishment of Na^+,K^+-ATPase polarity (11). Furthermore, in vivo ischemia leads to a rapid, duration-dependent disruption of the proximal tubule cell microfilament network (12).

Because Na^+,K^+-ATPase is directly linked to the actin membrane cytoskeleton, it is plausible to suggest that its movement from the basolateral membrane into the apical membrane domain involves dissociation from the membrane-cytoskeletal complex. To investigate this hypothesis directly, a model of in vitro cellular ATP depletion was developed in $LLCPK_1$ cells. The effect of ATP depletion on the association of Na^+,K^+-ATPase with the membrane-cytoskeleton was quantified by separating cell extracts into Triton-X-100–soluble and -insoluble (cytoskeletal) fractions. The effects of cellular ATP depletion on microfilament disruption and the state of actin polymerization was investigated by biochemical and immunocytochemical methods.

Methods

Cells. A cloned line of $LLCPK_1$ cells was obtained by limiting dilution, plated at 1×10^6 cells/60-mm dish and grown in DMEM containing 4% FCS and 4% calf serum. Unless otherwise indicated all studies were performed on monolayers that had reached confluence 48–72 h before the study. To induce cellular ATP depletion, monolayers were rinsed twice with PBS and then DMEM devoid of amino acids and glucose, but containing 1.5 μM antimycin A, was added (13).

Cell extraction, fractionation, and measurement of Na^+,K^+-ATPase activity. Confluent monolayers of $LLCPK_1$ cells in 60-mm dishes were transferred to 4°C, rinsed twice with PBS, and then solubilized and extracted using 200 μl of a PHEM buffer (60 mM Pipes, 25 mM Hepes, 10 mM EGTA, and 2 mM $MgCl_2$, pH 6.9, containing 0.1% Triton-X-100, 0.5 mM PMSF, and 0.1 mM DTT). Cells were extracted for 5 min on a rocking platform, cell residues were scraped from the petri dish with a rubber policeman, and pelleted at 48,000 *g* for 5 min at 4°C. Supernatants were carefully separated and pellets were resuspended in 200 μl of the PHEM extraction buffer. Na^+,K^+-ATPase activity was measured kinetically on extracted cells, supernatants and pellets as the difference between total and ouabain-inhibitable ATPase activity using

Address correspondence to Bruce A. Molitoris, M.D., Denver VA Medical Center (111C), 1055 Clermont St., Denver, CO 80220.

Received for publication 3 January 1991 and in revised form 27 March 1991.

1. *Abbreviations used in this paper:* BLM, basolateral membrane; MDCK, Madin-Darby canine kidney.

J. Clin. Invest.

0021-9738/91/08/0462/08 $2.00
Volume 88, August 1991, 462–469

an assay system coupled to pyruvate kinase, phosphoenolpyruvate, and lactate dehydrogenase at 340 nm and 37°C (14). For all assays, 50–150 μg of protein was used and assays were done in duplicate. Previous investigations have shown that the pellet consists primarily of the cellular cytoskeleton and associated proteins, whereas the supernatant consists of soluble proteins including G-actin and proteins which are capable of interacting with the cytoskeleton (for example, fodrin) but which were not associated with the cytoskeleton at the time of extraction (2–4). In our studies, cellular ATP depletion did not alter the Coomassie-blue SDS-PAGE protein profile of either the supernatant or pellet fractions (data not shown), except there was a decrease in the intensity of the G-actin band during ATP depletion. Proteins were determined by the technique of Lowry et al. (15) using BSA as a standard. Protein and Na^+,K^+-ATPase recovery were 100%.

Monomeric and filamentous actin determinations. The total amount of cellular actin and the fraction that was monomeric G-actin in $LLCPK_1$ cells were determined, utilizing the DNase I assay at 25° as described by Blikstad et al. (16) and modified by Laub et al. (17) and Podolski and Steck (18). For total cellular actin, confluent monolayers were transferred rapidly to 4°C, washed twice with ice-cold PBS, extracted in 400 μl of an actin-dissociating buffer (2 mM Tris-Cl, 0.2 mM Na_2ATP, 0.5 mM 2-mercaptoethanol, 0.2 mM $CaCl_2$, and 0.005% azide at pH 8.0) containing 0.5% Triton-X-100, 0.5 mM PMSF, 0.1 mM DTT, 0.01 mg/ml chymostatain, 0.01 mg/ml leupeptin, and 0.05 mg/ml *N-p*-tosyl-lysine chloromethyl ketone for 5 min at 4°C, scraped off the petri dish with a rubber policeman and allowed to depolymerize on ice for 3 h. For G-actin, monolayers were extracted with 200-μl of PHEM containing 0.5 mM PMSF, 0.5% Triton-X-100, and 0.1 mM DTT with gentle rocking at 4°C for 5 min, centrifuged for 5 min at 48,000 *g*, and the supernatant was immediately separated from the pellet. Monomeric actin concentrations in these samples were determined by quantifying the inhibition of hydrolysis of calf thymus DNA (Sigma Chemical Co., St. Louis, MO) by known amounts of pancreatic DNase I, utilizing the decrease in fluorescence of ethidium bromide (0.4 mg/ml). Fluorescence was measured with a spectrofluorometer (LS-3; Perkin-Elmer Corp., Norwalk, CT) at an excitation wave length of 520 nm and emission wavelength of 602 nm. Standard actin inhibition curves were generated utilizing actin (Sigma Chemical Co., St. Louis, MO) that was depolymerized in the dissociation buffer just before its use. Only values falling between 25 and 75% inhibition of the DNase I activity were used for quantitation (16–18).

Fluorescent staining of cells. For immunofluorescence labeling of Na^+,K^+-ATPase, monolayers of $LLCPK_1$ cells grown on 12-mm No. 1 circular glass coverslips (Bellco Glass Inc., Vineland, NJ) were washed in PBS and fixed with either methanol (−20°C for 5 min) followed by acetone (−20°C for 5 min) and then rinsed in PBS or with 4% freshly prepared paraformaldehyde and 0.1% glutaraldehyde in PME (60 mM Pipes, 2 mM $MgCl_2$, and 10 mM EGTA) buffer. Cells were then treated with 50% nonspecific goat serum in PBS for 60 min at 37°C followed by application of a monospecific polyclonal antibody (2, 6) to the α subunit of Na^+,K^+-ATPase (NKA 2.2 kindly provided by W. J. Nelson) at a dilution of 1:100 (PBS with 10% goat serum) for 60 min at 37°. This was followed by three rinses in PBS and application of a Texas Red–conjugated goat anti–rabbit IgG (Fisher Scientific Co., Fairlawn, NJ) diluted 1:500 (PBS with 10% goat serum) for 1 h at 37°. Coverslips were mounted in Gelvatol (Monsanto, Indian Orchard, MA) with 5% *n*-propyl gallate. The aldehyde fixed cells were dehydrated for 5 min in increasing concentrations of acetone and then embedded in Epon-Araldite (19). Lateral sections (0.5 μm) were cut, mounted, and viewed through a Zeiss Universal microscope equipped with a 50-W mercury arc, epifluorescence optics, a 100×, 1.25NA plan acromatic objective (Carl Zeiss, Inc., Thornwood, NY) and photographed on TMZ-P3200 film (Eastman Kodak Co., Rochester, NY).

Rhodamine-phalloidin (Molecular Probes, Inc., Eugene, OR) was utilized for labeling filamentous actin. Cells grown on glass cover slips were fixed in 3.7% formaldehyde, extracted with acetone (−20°C) and stained with a 1:10 dilution (PBS) of the rhodamine phalloidin as described by the product insert. Nuclear labeling was accomplished by exposing cells to 4,6-diamidino-2-phenylindole (DAPI) during the final PBS wash followed by a brief rinse in distilled H_2O. Statistical comparisons between control and experimental groups were made using analysis of variance (ANOVA), with results considered statistically different if the P value was < 0.05, and are reported as $P < 0.05$, $P < 0.01$ or NS. All values are reported as the mean±SD.

Cellular ATP measurements. ATP determinations were carried out on neutralized perchloric acid (PCA) extracts as previously described (13). Briefly, monolayers of $LLCPK_1$ cells were rinsed twice with PBS and extracted with 6% PCA at 4°C for 15–60 min. The PCA extract was neutralized with K_2CO_3. ATP was measured fluorimetrically with a luciferase assay using a monolight 2010 luminometer (Analytical Luminescence Laboratory, San Diego, CA).

Results

In MDCK cells the establishment of a polar distribution of Na^+,K^+-ATPase coincides temporally and spatially with the establishment of extensive cell–cell contact and the formation of a cortical cytoskeletal complex (6, 7). To investigate whether the same is true of $LLCPK_1$ cells, we determined whether the expression of Na^+,K^+-ATPase activity in this cell type was dependent upon the level of cellular confluence. Fig. 1, A–C, shows rhodamine phalloidin staining of filamentous actin in $LLCPK_1$ cells at different stages of confluence. Fig. 1 *D* displays the activity of Na^+,K^+-ATPase in the detergent-soluble (*solid circles*) and detergent-insoluble (*open circles*) fractions. The activity shown at 24, 48, and 72 h corresponds to cells at the level of confluences shown in Fig. 1, *A–C,* respectively. Cells that were less than ~ 70% confluent showed numerous stress fibers and a very small amount of cortical (surface membrane–associated) filamentous (F)–actin staining. After the establishment of cellular confluence, there was a marked reduction in the number of stress fibers and an increase in the cortical localization of F-actin staining. This process progressed for an additional 24 h after the establishment of confluence, and no stress fibers were detectable in the mature monolayer. Actin redistribution was associated with a marked increase in the activity of Na^+,K^+-ATPase. In the nonconfluent state, cellular Na^+,K^+-ATPase activity was only 0.33 μmol/mg protein per h, and the activity was almost uniformly distributed between the detergent-soluble and -insoluble fractions. With the establishment of monolayer confluence, there was a marked increase in the detergent-insoluble Na^+,K^+-ATPase activity, whereas the soluble form of Na^+,K^+-ATPase remained unchanged. After an additional 24 h at confluence, there was a further marked increase in the Na^+,K^+-ATPase activity in the detergent-insoluble fraction of Na^+,K^+-ATPase activity with no change in the amount of nonassociated Na^+,K^+-ATPase activity. During the establishment of cellular confluence in $LLCPK_1$ cells, cellular Na^+,K^+-ATPase activity increased from 0.33 to 1.80 μmol/mg protein per h, and the detergent-insoluble fraction increased from 0.22 to 1.74 μmol/mg protein per h. Therefore, establishment of confluence in $LLCPK_1$ cells is followed by the marked accumulation and redistribution of Na^+,K^+-ATPase from the soluble to the insoluble fraction.

The effect of cellular ATP depletion on the association between Na^+,K^+-ATPase and the cortical cytoskeleton was studied by placing fully confluent monolayers of $LLCPK_1$ cells in DMEM devoid of glucose and amino acids but containing 1.5 μM antimycin A. Under these conditions cellular ATP de-

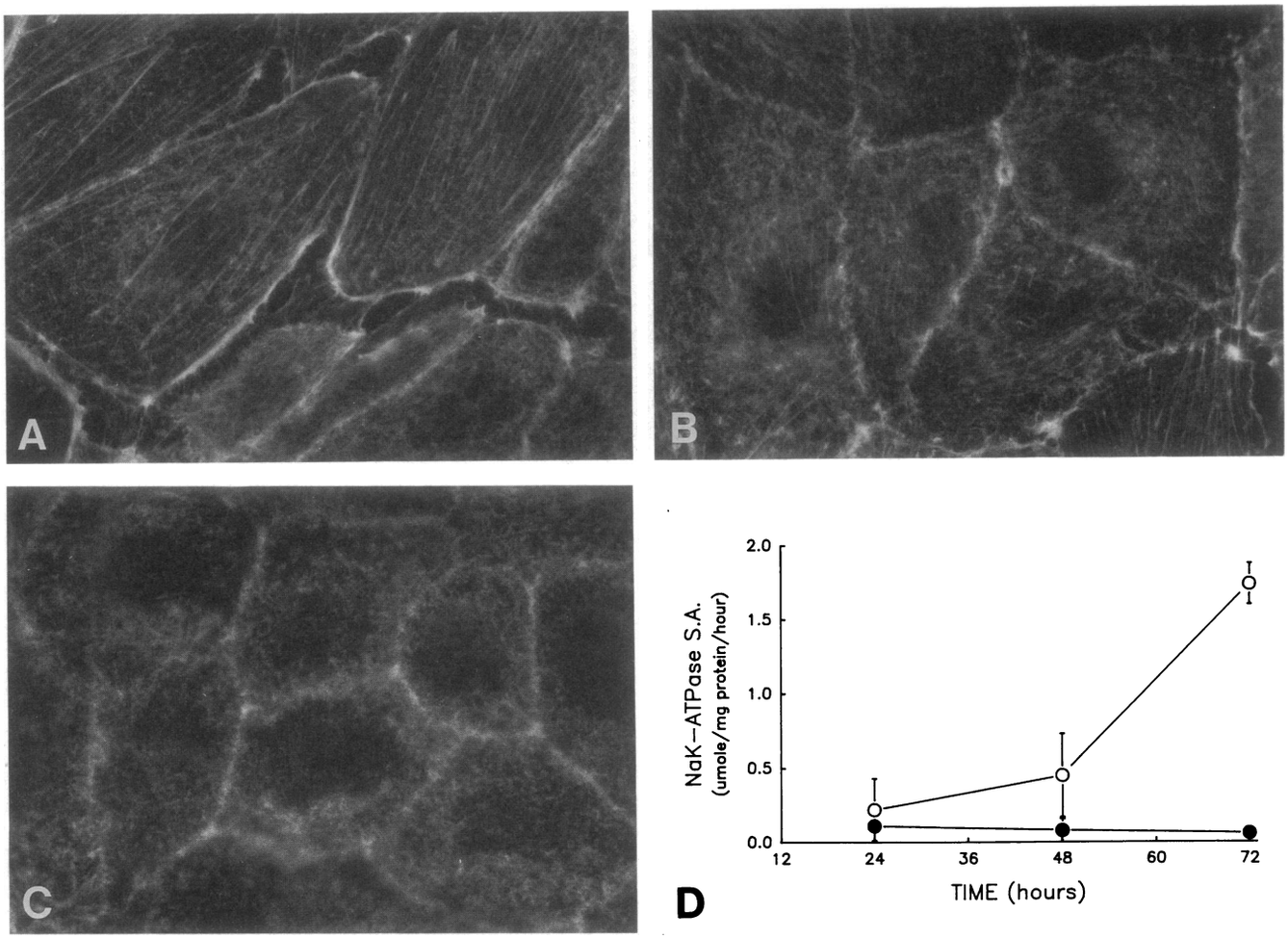

Figure 1. Immunofluorescent staining of F-actin in $LLCPK_1$ cells utilizing rhodamine phalloidin. $LLCPK_1$ cells were stained at different levels of confluence (*A*) 70% confluent; (*B*) early complete confluence; (*C*) mature confluent monolayer; (*D*) the specific activity of Na^+,K^+-ATPase for both detergent-soluble (noncytoskeletal associated [●]) and detergent-insoluble (cytoskeletal associated [○]) forms at times 24, 48, and 72 h after plating at 10^6 cells/60-mm dish. These times correspond to *A*, *B*, and *C*, respectively. n = 4 determinations done in duplicate for each data point. Magnification, 4,000.

clined rapidly from 8.62±0.59, under physiologic conditions, to 0.63±0.08 (7.3%) and 0.26±0.04 pmol/mg protein (3.0%) after 15 and 30 min exposure, respectively. After 60 and 120 min of exposure to substrate free media containing 1.5 μm antimycin A ATP was not detectable. These data are in agreement with previously published results using this model (13). Furthermore, culture media containing substrates and 1.5 μM antimycin A or media without either substrates or antimycin A did not result in ATP depletion, alterations in Na^+,K^+-ATPase distribution or rearrangement of the cortical actin cytoskeleton during the 120-min study period implying the effect was due to cellular ATP depletion. Cellular Na^+,K^+-ATPase activity remained constant during ATP depletion, but the activity redistributed among the detergent-soluble and -insoluble fractions (Fig. 2). 30 min of ATP depletion resulted in a statistically significant decrease in the amount of detergent insoluble Na^+,K^+-ATPase activity from (1.89±0.19 to 1.39±0.14 μmol/mg protein per h ($P < 0.01$). There was a corresponding in-

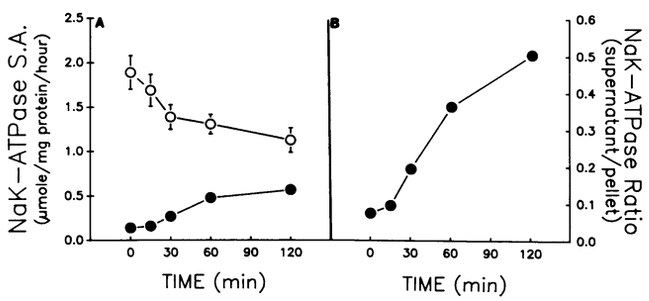

Figure 2. Dissociation of Na^+,K^+-ATPase from the cytoskeleton during cellular ATP depletion. Detergent-insoluble Na^+,K^+-ATPase (○) and detergent-soluble Na^+,K^+-ATPase (●) were determined under physiological conditions, and after increasing durations of cellular ATP depletion. *A* shows specific activities of the two fractions, whereas *B* shows the ratio of detergent-soluble to detergent-insoluble (supernatant/pellet) Na^+,K^+-ATPase. n = 8–13 determinations done in duplicate for each data point.

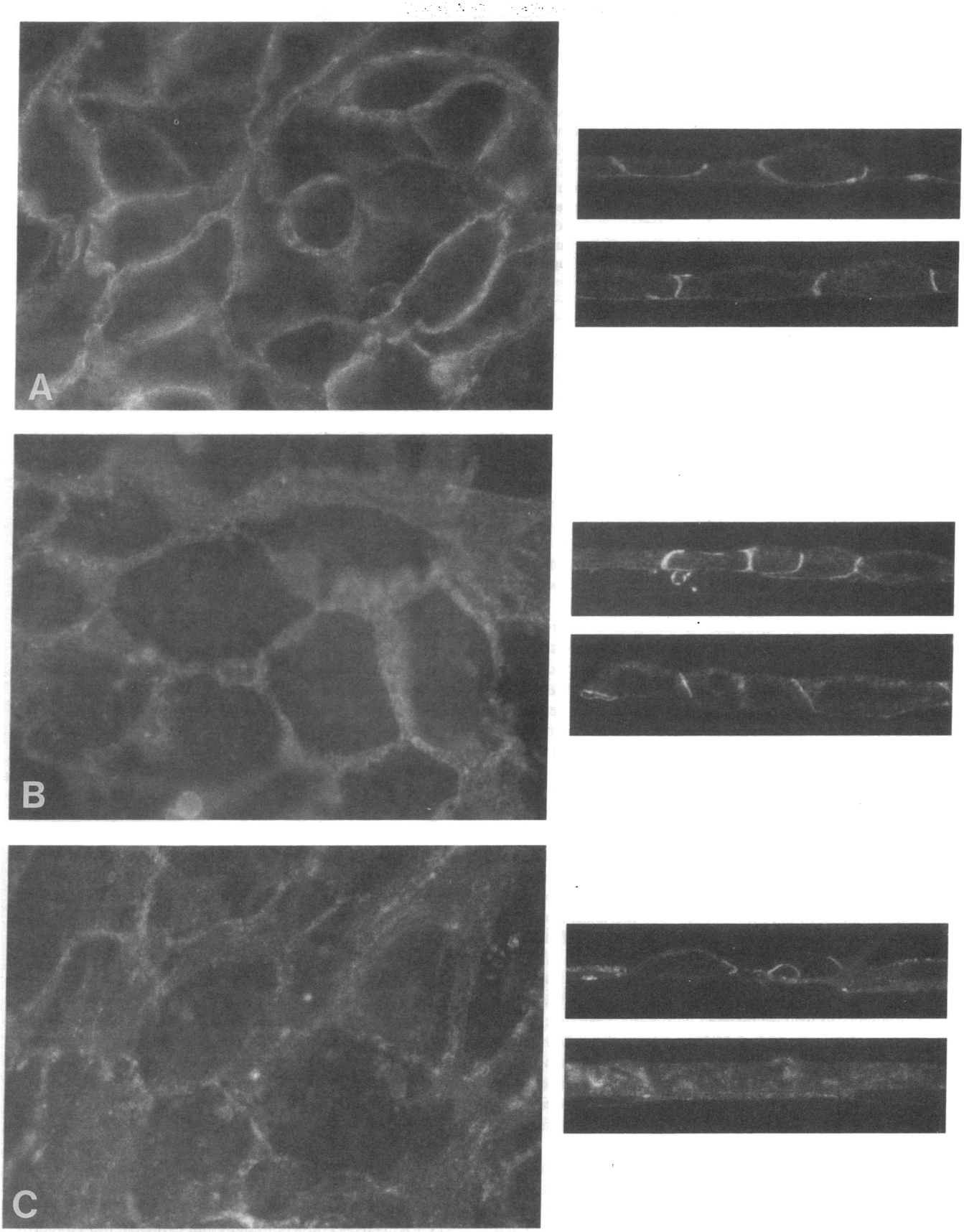

Figure 3. Effect of ATP depletion on the localization of Na^+,K^+-ATPase in $LLCPK_1$ cells, as seen by immunofluorescence. *A–C* portray cells under physiological conditions and after 1 and 2 h of cellular ATP depletion, respectively. Panels on left are the view looking down on the monolayer, whereas lateral views of upon embedded and sectioned cells are shown on right. Magnification, 4,000.

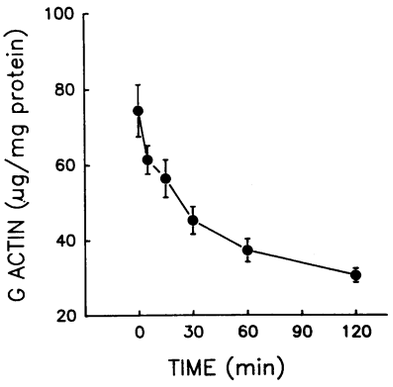

Figure 4. The effect of ATP depletion on cellular G-actin. Cellular monomeric actin was determined under physiological conditions and then after 5, 15, 30, 60, and 120 min of cellular ATP depletion utilizing the DNAse I assay. G-Actin is reported as micrograms per milligram protein in the supernatant. $n = 4$.

crease in Na^+,K^+-ATPase activity in the detergent-soluble fraction. Further redistribution of Na^+,K^+-ATPase activity from the detergent-insoluble fraction to the detergent-soluble fraction continued with increasing duration of cellular ATP depletion. After 120 min of ATP depletion, the activity of Na^+,K^+-ATPase in the detergent-soluble fraction had increased fourfold from 0.14±0.03 to 0.57±0.06 μmol/mg protein per h ($P < 0.01$) and the ratio of detergent-soluble to -insoluble Na^+,K^+-ATPase activity had increased from 0.074 to 0.504 ($P < 0.01$).

Indirect immunofluorescent studies were undertaken to determine the effect of cellular ATP depletion on the subcellular distribution of Na^+,K^+-ATPase. Under physiological conditions (Fig. 3 *A*), Na^+,K^+-ATPase was confined to the basolateral membrane domain, primarily its lateral component. After 60 min of ATP depletion Na^+,K^+-ATPase was detected in the apical membrane and a decrease in staining intensity was noted in the basolateral membrane (Fig. 3 *B*). 2 h of ATP depletion resulted in further increases in apical staining, and in some cells Na^+,K^+-ATPase was seen throughout the cytoplasm in a vesicular pattern (Fig. 3 *C*).

The redistribution of Na^+,K^+-ATPase from the detergent-insoluble to the detergent-soluble pool and from the BLM to throughout the cell suggested that ATP depletion was inducing a major change in cytoskeletal architecture resulting in a profound effect on cell polarity. Therefore, we assessed the effect of ATP depletion on the actin cytoskeleton through a biochemical determination of the state of actin polymerization utilizing the DNase I assay, and a cytochemical description of the F-actin (rhodamine phalloidin staining) distribution in $LLCPK_1$ cells. Total cellular actin (123±4 μg/mg cellular protein) remained stable as the cells progressed from a state of 50% cellular confluence to well-established confluent monolayers. The percentage of G-actin (34±1.5%) was also independent of the state of cell confluence. Therefore, progressing from a nonconfluent cell, whose actin consisted primarily of F-actin stress fibers, to a confluent cell with an abundant cortical actin cytoskeleton, had no effect on cellular actin concentration or the state of actin polymerization.

Depletion of cellular ATP did, however, result in the rapid conversion of G- to F-actin (Fig. 4). G-Actin diminished rapidly from a normal value of 74.4±6.9 to 30.6±1.9 (μg/mg supernatant protein) during 120 min of ATP depletion. There was no change in total cellular actin (data not shown). The decrease in G-actin was statistically significant after only 5 min of ATP depletion (from 74.4±6.9 to 61.4±3.8 μg/mg supernatant protein [$P < 0.01$]). Cellular G-actin continued to decrease rapidly for 30 min and then at a reduced rate for the rest of the 120-min period that we studied.

The conversion of G- to F-actin was associated with dramatic, duration-dependent alterations in the cellular distribution of F-actin. Under physiological conditions, the actin cytoskeleton was confined to a cortical distribution (Fig. 5 *A*). After 30 min of ATP depletion, small punctate dispersions of rhodamine phalloidin staining were seen throughout the cytoplasm (Fig. 5 *B*). Increasing the duration of ATP depletion to 120 min (Fig. 5, *C* and *D*) resulted in large cytoplasmic aggregates of rhodamine phalloidin staining and markedly decreased cortical staining. Fig. 5, *E* and *F*, show that the rhodamine phalloidin–stained aggregates were primarily localized to a perinuclear region.

To determine whether 2 h of ATP depletion resulted in irreversibly damaged cells, two studies were carried out. First, cellular LDH release was measured under physiological conditions and during 30, 60, and 120 min of ATP depletion. ATP depletion for up to 120 min had no effect on LDH release when compared with untreated cells (2.7% of total cellular LDH). Second, the ability of ATP-depleted cells to resynthesize ATP after substrate addition and antimycin removal was investigated. Cells that were ATP depleted for 120 min showed a rapid and sustained increase in cellular ATP when they were transferred back in to physiologic DMEM (Fig. 6). This increase in ATP correlated with the normalization of cellular morphology and actin distribution (data not shown).

Discussion

A polar distribution of Na^+,K^+-ATPase in renal proximal tubule cells is essential for the efficient reabsorption of Na^+ from the glomerular filtrate. Na^+,K^+-ATPase is synthesized in the endoplasmic reticulum, undergoes posttranslational modification in the Golgi apparatus and is targeted in a polar fashion to the BLM (1). There the enzyme associates with the cortical actin cytoskeleton via a specific linkage of the α subunit to ankyrin (4–6). This results in a metabolically stable cytoskeletal-enzyme complex which remains associated during Triton-X-100–mediated cellular disruption and extraction (4, 6, 7). In this paper, we have used cultured $LLCPK_1$ cells to investigate the effects of culture conditions and ATP depletion on the polar distribution of Na^+,K^+-ATPase and the F-actin cytoskeleton. We have demonstrated that the expression of Na^+,K^+-ATPase activity is dependent upon the establishment of a confluent monolayer and that this change is contemporaneous with the development of a mature cortical cytoskeleton. As confluence was established there was an increase in Na^+,K^+-ATPase activity that was restricted to the detergent-insoluble or cytoskeleton associated fraction of the cell, and the detergent-soluble or noncytoskeletal Na^+,K^+-ATPase fraction remained essentially unchanged. These findings are consistent with previously published data which indicate that the expression and establishment of Na^+,K^+-ATPase polarity coincides with the organization of the actin-fodrin-ankyrin-uvomorulin surface membrane-cytoskeletal complex (7).

The reorganization of the actin cytoskeleton that occurs as $LLCPK_1$ cells become confluent and express a more polarized phenotype is quite dramatic. Initially, the large, flat, nonconfluent $LLCPK_1$ cells had an actin cytoskeleton consisting primarily of stress fibers with little or no cortical structure appar-

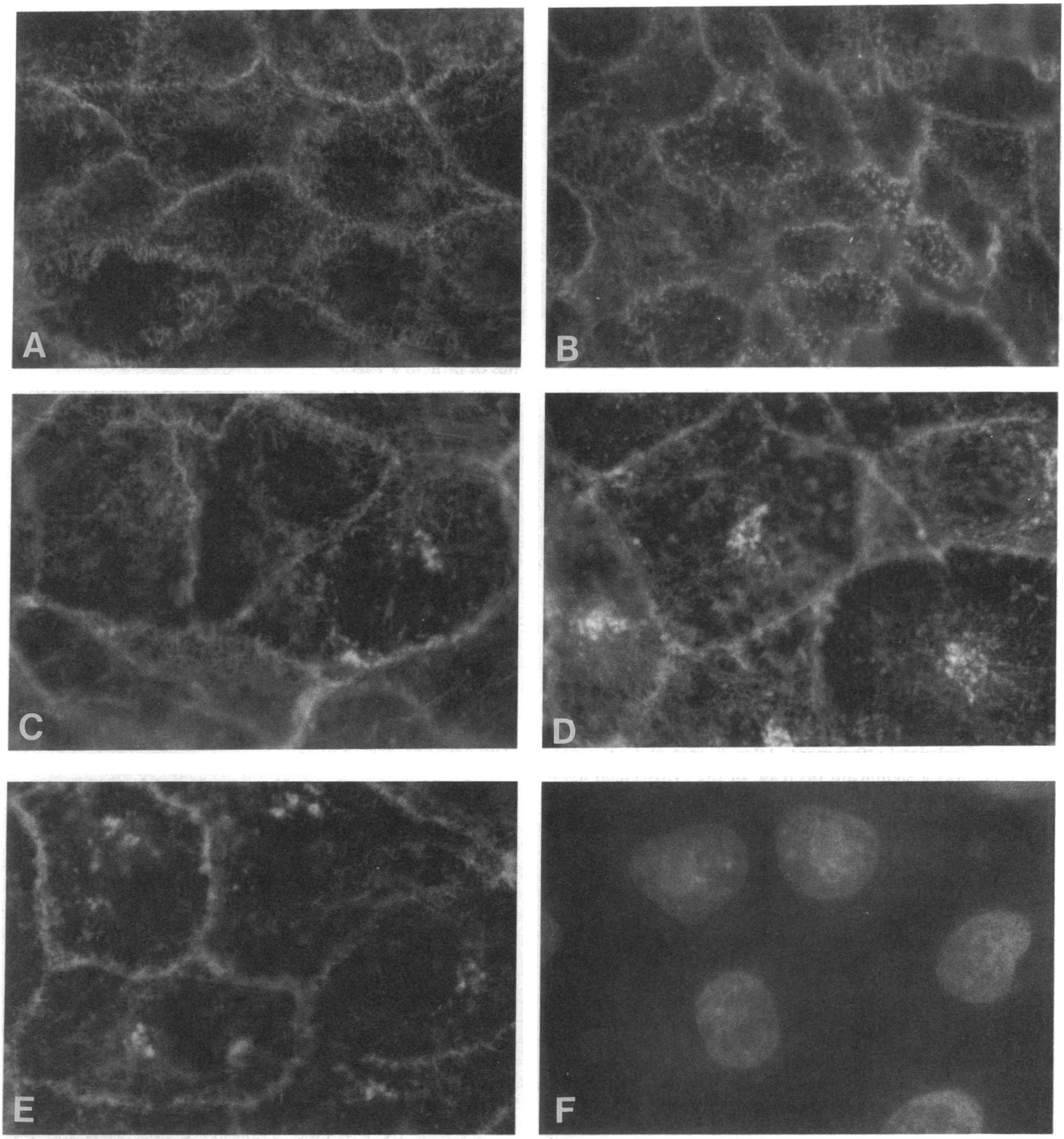

Figure 5. Effect of ATP depletion on the distribution of filamentous actin in $LLCPK_1$ cells. Filamentous actin was stained using rhodamine phalloidin under physiological conditions and after 30 (*B*), 60 (*C*), and 120 (*D, E*) min of cellular ATP depletion. *F* is the same focal plane as *E* and shows the nuclear staining (DAPI) of the cells shown in *E*.

ent. As the cells became confluent there was a progressive rearrangement of the actin cytoskeleton to a surface membrane association. These alterations were independent of any change in the extent of intracellular actin polymerization, as the percentage of G-actin remained constant. Our observations are consistent with results from MDCK cells (2) although the constancy of the G-actin percentage before and after the establishment of confluence has not been previously reported.

Our results also characterize some of the effects of ATP depletion on confluent monolayers of $LLCPK_1$ cells. Both Na^+,K^+-ATPase and the phalloidin-binding component of the actin cytoskeleton redistribute. Previous in vivo studies have documented the redistribution of Na^+,K^+-ATPase into the apical membrane during ischemic cell injury (8, 9). Because ischemia results in the rapid duration-dependent opening of proximal tubule cell tight junctions (20), we have postulated that

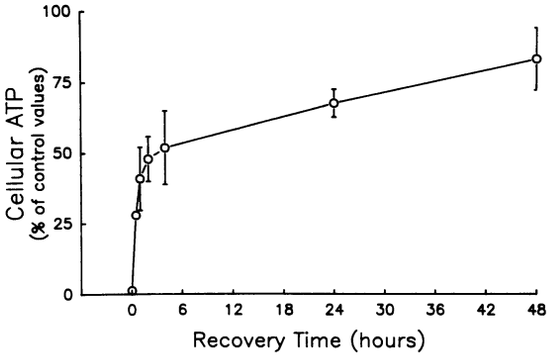

Figure 6. Reversibility of cellular ATP after 120 min of ATP depletion. Monolayers of $LLCPK_1$ cells were incubated in substrate free media containing 1.5 μM antimycin A for 120 min, carefully washed with PBS three times and then DMEM containing calf and fetal calf serum was added. ATP was measured at the times indicated during the recovery period. ATP was expressed as a percent of untreated cellular levels due to the variability in untreated cellular values which ranged from 4.6±0.5 to 7.3±1.7 pmol/mg protein. All values represent the mean±SD of n = 4–5 determinations done in duplicate.

Na^+,K^+-ATPase redistribution occurs via lateral bilayer movement through an open tight junction (20). However, under physiological conditions the lateral migration of Na^+,K^+-ATPase within the bilayer is limited by its cytoskeletal attachment. Therefore, a prerequisite for the validity our hypothesis is the dissociation of Na^+,K^+-ATPase from its cytoskeletal attachments. The work presented here has demonstrated that this prerequisite is fulfilled. Cellular ATP depletion resulted in the rapid, duration-dependent dissociation of Na^+,K^+-ATPase from its cytoskeletal attachment. After 30 min of ATP depletion there was a significant decrease in the cytoskeletal associated (detergent-insoluble) Na^+,K^+-ATPase fraction. During ATP depletion, there was no change in total cellular Na^+,K^+-ATPase activity, but, the ratio of noncytoskeletal to cytoskeletal associated Na^+,K^+-ATPase increased greater than sevenfold.

During ATP depletion, Na^+,K^+-ATPase was found to redistribute to the apical pole of individual $LLCPK_1$ cells. Apical membrane Na^+,K^+-ATPase staining was first noted after 1 h of ATP depletion, and continued ATP depletion resulted in increased apical staining. These data are consistent with our previous in vivo proximal tubule results where the rapid duration-dependent redistribution of Na^+,K^+-ATPase to the apical membrane during ischemic injury has been documented (9, 20). Furthermore, the time course for the opening of cellular tight junctions in vivo and in vitro (preliminary data in $LLCPK_1$ cells; 21) is consistent with the lateral bilayer mobility of noncytoskeletal associated basolateral membrane Na^+,K^+-ATPase into the apical membrane through an open tight junction.

Previous results from our laboratory have indicated that apically localized Na^+,K^+-ATPase retains its functional ability and is, in part, responsible for reduced and inefficient Na^+ reabsorption after ischemic cell injury (10). Furthermore, repolarization of the Na^+,K^+-ATPase distribution to the BLM is required before proximal tubule Na^+ reabsorption can normalize (11).

Dissociation of Na^+,K^+-ATPase from its cytoskeletal attachment was preceded by the rapid conversion of G- to F-actin and the redistribution of filamentous actin from a cortical to a perinuclear location. The mechanism for conversion of G- to F-actin was not further investigated, but poses an interesting puzzle. Actin polymerization in vitro requires ATP (22), so the mechanism by which ATP depletion enhances the formation of F-actin in cells is not obvious. The result may, of course, be an artifact of the experimental definitions of G and F actin used, but we think it likely that the redistribution is real and results from the wide-ranging effects that ATP depletion may have on the levels of phosphorylation in actin binding proteins. While the mechanisms by which 30–50% of cellular actin is kept soluble are complex and still obscure (23), it seems likely that the supramolecular organization of actin into a cortical network involves a complex of dynamic protein–protein interactions that would be sharply altered by changes in the activities of protein kinases.

In summary, ATP depletion in $LLCPK_1$ cells results in a rapid duration-dependent conversion of G- to F-actin, redistribution of actin from a cortical to perinuclear localization, dissociation of the Na^+,K^+-ATPase-cytoskeletal complex and a redistribution of Na^+,K^+-ATPase to the apical membrane. These data are consistent with and extend previous in vivo observations. They support the hypothesis that ischemia results in loss of surface membrane polarity by disrupting the actin cytoskeleton which in turn leads to a dissociation of cytoskeleton associated proteins and the opening of tight junctions. Lateral migration of domain specific components could then occur, resulting in loss of surface membrane polarity.

Acknowledgments

This work was supported by grants to Dr. Molitoris from the National Institutes of Health DK-41126 and the Veterans Affairs Research Service. Dr. Molitoris is the recipient of a Clinical Investigator Award from the Veterans Affairs Research Service.

References

1. Caplan, M. J., H. C. Anderson, G. E. Palade, and J. D. Jamieson. 1986. Intracellular sorting and polarized cell surface delivery of (Na^+,K^+)ATPase, an endogenous component of MDCK cell basolateral plasma membranes. *Cell.* 46:623–631.

2. Nelson, W. J., and P. J. Veshnock. 1986. Dynamics of membrane-skeleton (fodrin) organization during development of polarity in Madin-Darby canine kidney epithelial cells. *J. Cell Biol.* 103:1751–1765.

3. Nelson, W. J., and P. J. Veshnock. 1987. Modulation of fodrin (membrane skeleton) stability by cell-cell contact in Madin-Darby canine kidney epithelial cells. *J. Cell Biol.* 104:1527–1537.

4. Nelson, W. J., and P. J. Veshnock. 1987. Ankyrin binding to Na^+,K^+-ATPase and implications for the organization of membrane domains in polarized cells. *Nature (Lond.).* 328:533–536.

5. Morrow, J. S., C. D. Cianci, T. Ardito, A. S. Mann, and M. Kashgarian. 1989. Ankyrin fodrin to the α subunit of Na^+,K^+-ATPase in Madin-Darby canine kidney cells in intact renal tubule cells. *J. Cell Biol.* 108:455–465.

6. Nelson, W. J., and R. W. Hammerton. 1989. A membrane-cytoskeletal complex containing Na^+,K^+-ATPase, ankyrin, and fodrin in Madin-Darby canine kidney (MDCK) cells: implications for the biogenesis of epithelial cell polarity. *J. Cell Biol.* 108:893–902.

7. Nelson, W. J., E. M. Shore, A. Z. Wang, and R. W. Hammerton. 1990. Identification of a membrane-cytoskeletal complex containing the cell adhesion molecule uvomorulin (E-cadherin), ankyrin and fodrin in Madin-Darby canine kidney (MDCK) epithelial cells. *J. Cell Biol.* 110:349–357.

8. Molitoris, B. A., P. D. Wilson, R. W. Schrier, and F. R. Simon. 1985. Ischemia induces partial loss of surface membrane polarity and accumulation of putative calcium ionophores. *J. Clin. Invest.* 76:2097–2105.

9. Molitoris, B. A., C. A. Hoilien, R. H. Dahl, D. J. Ahnen, P. D. Wilson, and J. Kim. 1988. Characterization of ischemia-induced loss of epithelial polarity. *J. Membr. Polarity.* 106:233–242.

10. Molitoris, B. A., L. K. Chan, J. I. Shapiro, J. D. Conger, and S. A. Falk. 1989. Loss of epithelial polarity: a novel hypothesis for reduced proximal tubule Na^+ transport following ischemic injury. *J. Membr. Biol.* 107:119–127.

11. Spiegel, D. M., P. D. Wilson, and B. A. Molitoris. 1989. Epithelial polarity following ischemia: a requirement for normal cell function. *Am. J. Physiol. (Renal Electrolyte Physiol.).* 256:F430–F436.

12. Kellerman, P. S., R. A. F. Clark, C. A. Hoilien, S. L. Linas, and B. A. Molitoris. 1990. Role of microfilaments in the maintenance of proximal tubule structural and functional integrity. *Am. J. Physiol. (Renal Electrolyte Physiol.).* 259:F279–F285.

13. Venkatachalam, M. A., Y. J. Patel, J. I. Kreisberg, and J. M. Weinberg. 1988. Energy threshold that determine membrane integrity and injury in a renal epithelial cell line ($LLCPK_1$). Relationship to phospholipid degradation and unesterified fatty acid accumulation. *J. Clin. Invest.* 81:745–758.

14. Molitoris, B. A., and F. R. Simon. 1985. Renal cortical brush border and basolateral membranes: cholesterol and phospholipid composition and relative turnover. *J. Membr. Biol.* 83:207–215.

15. Lowry, O. H., N. J. Rosebrough, A. L. Farr, and R. J. Randall. 1951. Protein measurement with the fodrin phenol reagent. *J. Biol. Chem.* 193:256–275.

16. Blikstad, I., F. Markey, L. Carlsson, T. Persson, and U. Lindberg. 1978. Selective assay of monomeric and filamentous actin in cell extracts, using inhibition of deoxyribonuclease 1. *Cell.* 15:935–943.

17. Laub, F., M. Kaplan, and C. Glitlerc. 1981. Actin polymerization accompanies Thy-1-capping on mouse thymocytes. *FEBS (Fed. Eur. Biochem. Soc.) Lett.* 124:35–38.

18. Podolski, J. L., and T. L. Steck. 1990. Length distribution of F-actin in dictoyostelium discoideum. *J. Biol. Chem.* 265:1312–1318.

19. Rieder, C. L., and S. S. Bowser. 1985. Correlative immunofluorescence and electron microscopy on the same section of epon-embedded material. *J. Histochem. Cytochem.* 33:165–173.

20. Molitoris, B. A., R. H. Dahl, and S. A. Falk. 1989. Ischemic-induced loss of epithelial polarity. Role of the tight junction. *J. Clin. Invest.* 84:1334–1339.

21. Canfield, P. E., A. Geerdes, and B. A. Molitoris. 1990. Reversible cellular ATP depletion opens tight junctions. *J. Am. Soc. Nephrol.* 1:594A. (Abstr.)

22. Korn, E. O., M. F. Carlier, and D. Pantaloni. 1987. Actin polymerization and ATP hydrolysis. *Science (Wash. DC).* 238:636–644.

23. Sander, M. C., and Y. L. Wang. 1990. Exogenous nucleation sites fail to induce detectable polymerization of actin in living cells. *J. Cell Biol.* 110:359–365.